

# Accurate Nonempirical Correlation Energy Functional for Uniform Electron Gas

Qing-Xing Xie,<sup>1</sup> Jiashun Wu<sup>1</sup> and Yan Zhao<sup>1,2\*</sup>

<sup>1</sup>The Institute of Technological Sciences, Wuhan University, Wuhan 430072, People's Republic of China.

<sup>2</sup>State Key Laboratory of Silicate Materials for Architectures, International School of Materials Science and Engineering, Wuhan University of Technology, Hubei, Wuhan 430070, People's

\*Corresponding author, E-mail: [yan2000@whut.edu.cn](mailto:yan2000@whut.edu.cn)

## Abstract

We report an analytical representation of the correlation energy  $e_c(r_s, \zeta)$  for a uniform electron gas (UEG), where  $r_s$  is the Seitz radius or density parameter and  $\zeta$  is the relative spin polarization. The new functional, called W20, is constructed to capture the known high-density ( $r_s \rightarrow 0$ ) and low-density ( $r_s \rightarrow \infty$ ) limit (for  $\zeta = 0$  and 1) without any fitting parameters. The comparative assessment against the recent quantum Monte Carlo (QMC) results shows that the performance of the nonempirical W20 functional is comparable to the popular parametrized UEG correlation functionals. On average, W20 agrees with QMC and PW92 [[Phys. Rev. B 45, 13244 \(1992\)](#)] within 0.01 eV.

Since the birth of density functional theory (DFT) [1,2], the hypothetical uniform electron gas (UEG) has served as a ubiquitous model for the developments of density functionals, and all modern DFT calculations involve UEG-based components in the underlying exchange-correlation functionals. Although the analytical representation of the UEG exchange energy is known [3], the UEG correlation energy per electron,  $e_c(r_s, \zeta)$ , does not have a closed analytical form. Here, the Seitz radius,  $r_s$ , is related to the electron density  $\rho$  as

$$\rho = \rho_\uparrow + \rho_\downarrow = \left[ \frac{4\pi}{3} (r_s a_B)^3 \right]^{-1}, \quad (1)$$

where  $\rho_\uparrow$  and  $\rho_\downarrow$  are the up- and down-spin electron densities, respectively.  $a_B$  is the Bohr radius  $= \hbar/(me^2)$ , and the atomic units are employed ( $\hbar = m = e^2 = 1$ ).  $\zeta$  is the relative spin polarization,

$$\zeta = \frac{\rho_\uparrow - \rho_\downarrow}{\rho}. \quad (2)$$

The widely used VWN80 [4], PZ81 [5], and PW92 [6] UEG correlation functionals have been developed by parametrizing and interpolating between the discrete quantum Monte Carlo (QMC) data of Ceperley and Alder [7]. Inspired by the Wigner [8] interpolation, Sun, Perdew, and Seidl [9] recently proposed a density parameter interpolation (DPI) between the high-density ( $r_s \rightarrow 0$ ) and low-density ( $r_s \rightarrow \infty$ ) limits of the UEG  $e_c(r_s, \zeta)$  without parametrization against the QMC data. Later, Loos and Gill [10] have found that one of the expansion coefficients used in the original DPI model was in error, and Bhattacharai *et al.* [11] corrected this error and compared the two DPI functionals to VWN80, PZ81, PW92, and the QMC data of Spink *et al.* [12], and they found that the corrected DPI model agrees with the original DPI within 0.001 eV, showing the robustness of the DPI approach.

In 2016, Chachiyo[13] developed an elegant nonempirical functional (it is named as C16 in this work) based on second-order Moller-Plesset perturbation theory, and is of the form:

$$e_c(r_s, \zeta = 0, 1) = a(\zeta) \ln(1 + \frac{b(\zeta)}{r_s} + \frac{b(\zeta)}{r_s^2}) \quad (3)$$

The parameters  $a(\zeta)$  and  $b(\zeta)$  ( $\zeta = 0, 1$ ) in Eq. (3) have been nonempirically derived from the leading coefficients  $a_0(\zeta)$  and  $b_0(\zeta)$  ( $\zeta = 0, 1$ ) in the high-density asymptotic expansion of  $e_c(r_s, \zeta)$  [9,14-17]:

$$\begin{aligned} e_c(r_s, \zeta) &= \sum_{n=0}^{\infty} [a_n(\zeta) \ln(r_s) + b_n(\zeta)] r_s^n \\ &= a_0(\zeta) \ln(r_s) + b_0(\zeta) + r_s [a_1(\zeta) \ln(r_s) + b_1(\zeta)] + \dots \quad (r_s \rightarrow 0) \end{aligned} \quad (4)$$

Later, Karasiev [18] introduced an empirical parameter into Eq. (3) by using the QMC data at  $r_s = 50$  (this model is named as revC16 in this work), and he showed that the performance of revC16 is better than C16 for the predictions of UEG correlation energies.

Due to the limited flexibility of Eq. (3), the C16 and revC16 models can only recover the leading  $a_0(\zeta)$  and  $b_0(\zeta)$  ( $\zeta = 0, 1$ ) coefficients in Eq. (4), but not the  $a_1(\zeta)$  and  $b_1(\zeta)$  ( $\zeta = 0, 1$ ) ones. Furthermore, neither of the two models recovers the low-density limit expansion of  $e_c(r_s, \zeta)$  [4,6,8,9,11,19]:

$$\begin{aligned} e_c(r_s, \zeta) &= \frac{f_0 - c_x(\zeta)}{r_s} + \frac{f_1}{r_s^{3/2}} + \frac{f_2 - c_x(\zeta)}{r_s^2} \\ &\quad + \sum_{n=3}^{\infty} \frac{f_n}{r_s^{1+n/2}} + e_{\text{exp}}(r_s, \zeta) \quad (r_s \rightarrow \infty) \end{aligned} \quad (5)$$

where  $f_0, f_1$ , and  $f_2$  are constant coefficients;  $c_x(\zeta)$  and  $c_s(\zeta)$  are spin scaling function for the UEG exchange energy and noninteracting kinetic energy, respectively [6,9]:

$$c_s(\zeta) = \frac{3}{10} \left( \frac{9\pi}{4} \right)^{2/3} \frac{1}{2} \left[ (1 + \zeta)^{5/3} + (1 - \zeta)^{5/3} \right], \quad (6)$$

$$c_x(\zeta) = -\frac{3}{4\pi} \left(\frac{9\pi}{4}\right)^{1/3} \frac{1}{2} \left[ (1+\zeta)^{4/3} + (1-\zeta)^{4/3} \right]. \quad (7)$$

The aim of this work is to construct an accurate nonempirical UEG correlation functional without parametrization, and the proposed functional will be referred to as “W20” (stands for Wuhan 2020). The W20 model recovers both the high- and low-density limits (Eqs. (4) and (5) for  $\zeta = 0, 1$ ). The exact or near-exact coefficients in Eqs. (4) and (5) are listed in TABLE I and are employed in W20. The derivations of these coefficients have been summarized in the advanced review of UEG by Loos and Gill [20].

In order to achieve the high- and low-density asymptotic behaviors of Eqs. (4) and (5), we choose

$$e_c(r_s, \zeta) = -\frac{a_0(\zeta)}{2} \ln \left[ 1 + \frac{D(r_s, \zeta)}{r_s} + \frac{E(r_s, \zeta)}{r_s^{3/2}} + \frac{F(r_s, \zeta)}{r_s^2} \right] + G(r_s, \zeta). \quad (8)$$

Here,

$$D(r_s, \zeta) = e^{-2b_0[\zeta]/a_0[\zeta]} - 2 \left( 1 - e^{-(r_s/100)^2} \right) \left( \frac{f_0 - c_x(\zeta)}{a_0(\zeta)} + \frac{1}{2} e^{-2b_0[\zeta]/a_0[\zeta]} \right), \quad (9)$$

$$E(r_s, \zeta) = -\frac{2 \left( 1 - e^{-(r_s/100)^2} \right) f_1}{a_0(\zeta)}, \quad (10)$$

$$F(r_s, \zeta) = e^{-2b_0[\zeta]/a_0[\zeta]} - 2 \left( 1 - e^{-(r_s/100)^2} \right) \left( \frac{f_2 - c_s(\zeta)}{a_0(\zeta)} + \frac{1}{2} e^{-2b_0[\zeta]/a_0[\zeta]} \right), \quad (11)$$

$$G(r_s, \zeta) = \frac{r_s}{1 + 10e^{(r_s/100)^2} r_s^{5/4}} \left[ -a_1(\zeta) \ln \left( 1 + \frac{1}{r_s} \right) + b_1(\zeta) \right]. \quad (12)$$

In the high-density limit  $r_s \rightarrow 0$ ,  $(1 - e^{-(r_s/100)^2}) \rightarrow 0$ ,  $D(r_s, \zeta) \rightarrow e^{-2b_0[\zeta]/a_0[\zeta]}$ ,  $E(r_s, \zeta) \rightarrow 0$ ,  $F(r_s, \zeta) \rightarrow e^{-2b_0[\zeta]/a_0[\zeta]}$ , and  $G(r_s, \zeta) \rightarrow r_s [-a_1(\zeta) \ln r_s + b_1(\zeta)]$ . Therefore,

$$\begin{aligned}
e_c(r, \zeta) &\rightarrow -\frac{a_0(\zeta)}{2} \ln \left[ 1 + \frac{e^{-2b_0[\zeta]/a_0[\zeta]}}{r_s} + \frac{e^{-2b_0[\zeta]/a_0[\zeta]}}{r_s^2} \right] + r_s [-a_1(\zeta) \ln r_s + b_1(\zeta)] \\
&\rightarrow -\frac{a_0(\zeta)}{2} \ln \left[ \frac{e^{-2b_0[\zeta]/a_0[\zeta]}}{r_s^2} \right] + r_s [-a_1(\zeta) \ln r_s + b_1(\zeta)] \\
&= a_0(\zeta) \ln(r_s) + b_0(\zeta) + r_s [a_1(\zeta) \ln(r_s) + b_1(\zeta)]. \tag{13}
\end{aligned}$$

Eq. (13) demonstrates that  $e_c(r_s, \zeta)$  recovers the high-density limit of Eq. (4).

$$\begin{aligned}
&\text{In the low-density limit } r_s \rightarrow \infty, (1 - e^{-(r_s/100)^2}) \rightarrow 1, D(r_s, \zeta) \rightarrow -\frac{2(f_0 - c_x(\zeta))}{a_0(\zeta)}, E(r_s, \zeta) \\
&\rightarrow -\frac{2f_1}{a_0(\zeta)}, F(r_s, \zeta) \rightarrow -\frac{2(f_2 - c_s(\zeta))}{a_0(\zeta)} \text{ and } F(r_s, \zeta) \rightarrow 0, \\
e_c(r_s, \zeta) &\rightarrow -\frac{a_0(\zeta)}{2} \ln \left[ 1 - \frac{2(f_0 - c_x(\zeta))}{a_0(\zeta)r_s} - \frac{2f_1}{a_0(\zeta)r_s^{3/2}} - \frac{2(f_2 - c_s(\zeta))}{a_0(\zeta)r_s^2} \right] \\
&\rightarrow -\frac{a_0(\zeta)}{2} \left[ -\frac{2(f_0 - c_x(\zeta))}{a_0(\zeta)r_s} - \frac{2f_1}{a_0(\zeta)r_s^{3/2}} - \frac{2(f_2 - c_s(\zeta))}{a_0(\zeta)r_s^2} \right] \\
&= \frac{f_0 - c_x(\zeta)}{r_s} + \frac{f_1}{r_s^{3/2}} + \frac{f_2 - c_s(\zeta)}{r_s^2}. \tag{14}
\end{aligned}$$

Eq. (14) confirms that the low-density limit, *i.e.* Eq. (5), has been recovered by  $e_c(r_s, \zeta)$  of Eq. (8).

Note that the exact form of  $b_1(\zeta)$  in Eq. (4) is not known, and only  $b_1(0)$  has been determined by Endo *et al.* [16], so the expressions for the spin-unpolarized ( $\zeta = 0$ ) and fully polarized ( $\zeta = 1$ ) cases in W20 are slightly different,

$$e_c^{\text{W20}}(r_s, 0) = -\frac{a_0(0)}{2} \ln \left[ 1 + \frac{D(r_s, 0)}{r_s} + \frac{E(r_s, 0)}{r_s^{3/2}} + \frac{F(r_s, 0)}{r_s^2} \right] + G(r_s, 0), \tag{15}$$

$$\begin{aligned}
e_c^{\text{W20}}(r_s, 1) = & -\frac{a_0(1)}{2} \ln \left[ 1 + \frac{D(r_s, 1)}{r_s} + \frac{E(r_s, 1)}{r_s^{3/2}} + \frac{F(r_s, 1)}{r_s^2} \right] \\
& + \frac{r_s}{1 + 10e^{(r_s/100)^2} r_s^{5/4}} \left[ -a_1(1) \ln \left( 1 + \frac{1}{r_s} \right) \right]. \tag{16}
\end{aligned}$$

As shown in Eq. (16), the  $b_1(1)$  term in  $G(r_s, 1)$  of Eq. (12) has been removed from  $e_c^{\text{W20}}(r_s, 1)$ , and the final expression for the W20 UEG correlation functional is given as

$$e_c^{\text{W20}}(r_s, \zeta) = e_c^{\text{W20}}(r_s, 0) + [e_c^{\text{W20}}(r_s, 1) - e_c^{\text{W20}}(r_s, 0)]f(\zeta), \tag{17}$$

where  $f(\zeta)$  is the spin interpolation function developed by von Barth and Hedin [21], and it has been employed in the PZ81 [5] UEG correlation functional,

$$f(\zeta) = \frac{(1+\zeta)^{4/3} + (1-\zeta)^{4/3} - 2}{2^{4/3} - 2}. \tag{18}$$

Figure 1 shows that the nonempirical W20 model approaches the high- and low-density limits correctly. In TABLE II, we compare the correlation energy per electron,  $e_c(r_s, \zeta)$ , calculated from C16 [13], revC16 [18], and W20 and the QMC results of Spink *et al.* [12]. Since Bhattacharai *et al.* [11] have suggested that the QMC results for  $r_s = 0.5$  in the work of Spink *et al.* might not be accurate, only the results for the ranges  $1 \leq r_s \leq 20$  are presented in TABLE II. For the  $r_s = 1$  ( $\zeta = 0, 1$ ) cases, W20 shows the larger deviation from the QMC results than C16 and revC16, whereas in most of the other cases W20 gives better agreements. In TABLE III, we report the mean signed errors (MSEs) and mean unsigned errors (MUEs) of seven UEG correlation functionals by using the QMC results ( $1 \leq r_s \leq 20$ ) of Spink *et al.* as references. W20 gives the lowest MUE for  $\zeta = 0$ , whereas PZ81 is the best performer for  $\zeta = 0.34, 0.66$ , and 1. If we use average MUE (AMUE) to evaluate the performances of the tested UEG correlation

functionals, PZ81 is the best performer, followed by W20, PW92, and VWN80. It is encouraging that the AMUEs of PZ81, W20, and PW92 are less than 0.01 eV. Among the three best-performing functionals, W20 is the only nonparametrized UEG correlation functional developed by the constraint-satisfying approach without any fitting parameters.

As shown in TABLE III, Karasiev's modification (revC16) of C16 reduce the AMUE by 0.007 eV. The performance of DPI is between C16 and revC16, and this might due to the questionable QMC results at  $r_s = 1$ . If the data for  $r_s = 1$  are excluded, the AMUEs for W20, DPI, revC16, and C16 are 0.007 eV, 0.011 eV, 0.013 eV, and 0.020 eV, respectively.

Since Bhattacharai *et al.* suggested that PW92 is more accurate than the QMC results for  $r_s < 2$ , we have calculated AMUEs by using the PW92 data as the references for the full range ( $0.5 \leq r_s \leq 20$ ), and the AMUEs for W20, DPI, revC16, and C16 are 0.009 eV, 0.010 eV, 0.020 eV, and 0.025 eV, respectively.

In conclusion, inspired by the recent C16 [13] and DPI [9] models, a nonempirical UEG correlation functional, W20, is constructed by interpolating the known exact or near-exact high- and low-density asymptotic limits of UEG  $e_c(r_s, \zeta)$  without any fitting parameters. The W20 model recovers the high- and low-density limits for  $\zeta = 0$  and 1, and the comparative assessments have shown that W20 agrees with QMC and PW92 within 0.01 eV on average.

We thank Wuhan University for financial support and computational resources.

## Reference

- [1] P. Hohenberg and W. Kohn, Phys. Rev. B **136**, B864 (1964).
- [2] W. Kohn and L. J. Sham, Physical Review **140**, 1133 (1965).
- [3] P. A. M. Dirac, Proceedings of the Cambridge Philosophical Society **26**, 376 (1930).
- [4] S. H. Vosko, L. Wilk, and M. Nusair, Can. J. Phys. **58**, 1200 (1980).
- [5] J. P. Perdew and A. Zunger, Phys. Rev. B **23**, 5048 (1981).
- [6] J. P. Perdew and Y. Wang, Phys. Rev. B **45**, 13244 (1992).
- [7] D. M. Ceperley and B. J. Alder, Phys. Rev. Lett. **45**, 566 (1980).
- [8] E. Wigner, Physical Review **46**, 1002 (1934).
- [9] J. Sun, J. P. Perdew, and M. Seidl, Phys. Rev. B **81**, 085123 (2010).
- [10] P.-F. Loos and P. M. W. Gill, Phys. Rev. B **84**, 033103 (2011).
- [11] P. Bhattacharai, A. Patra, C. Shahi, and J. P. Perdew, Phys. Rev. B **97**, 195128 (2018).
- [12] G. G. Spink, R. J. Needs, and N. D. Drummond, Phys. Rev. B **88**, 085121 (2013).
- [13] T. Chachiyo, J. Chem. Phys. **145**, 021101 (2016).
- [14] M. Gellmann and K. A. Brueckner, Physical Review **106**, 364 (1957).
- [15] W. J. Carr and A. A. Maradudin, Physical Review a-General Physics **133**, A371 (1964).
- [16] T. Endo, M. Horiuchi, Y. Takada, and H. Yasuhara, Phys. Rev. B **59**, 7367 (1999).
- [17] P. Ziesche and J. Czoski, Physica a-Statistical Mechanics and Its Applications **356**, 598 (2005).
- [18] V. V. Karasiev, J. Chem. Phys. **145**, 157101 (2016).
- [19] W. J. Carr, R. A. Coldwellhorsfall, and A. E. Fein, Physical Review **124**, 747 (1961).
- [20] P.-F. Loos and P. M. W. Gill, WIREs Comput Mol Sci **6**, 410 (2016).
- [21] U. von Barth and L. Hedin, Journal of Physics C **5**, 1629 (1972).

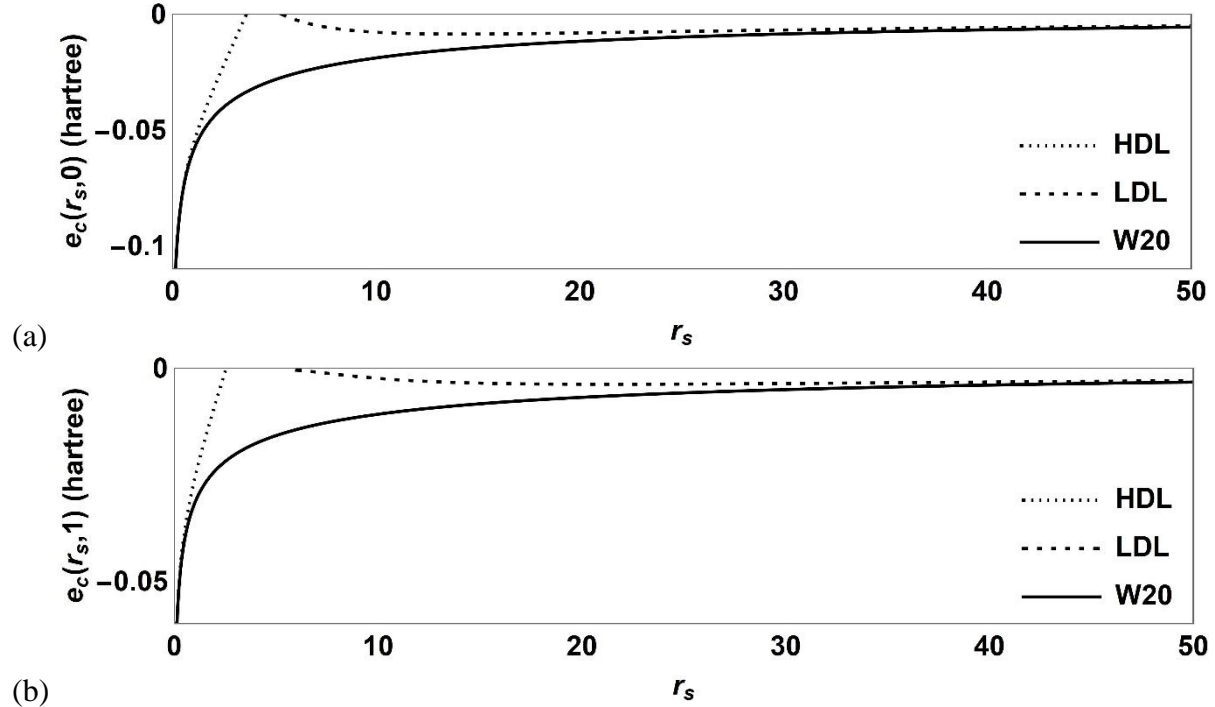


FIG. 1.  $e_c(r_s, \zeta=0, 1)$  vs  $r_s$  for the high-density limit (HDL, Eq. (4)) and the low-density limit (LDL, Eq. (5)) and the W20 model defined in Eqs. (15), (16), and (17). For  $e_c(r_s, 1)$ , the HDL curve does not have the  $b_1(1)$  term.

TABLE I. The exact or near-exact coefficients (in hartree) of the high-density ( $r_s \rightarrow 0$ ) and low-density ( $r_s \rightarrow \infty$ ) limit (for spin polarization  $\zeta=0$  and 1) of the UEG correlation energy in W20.  $z(n)$  is the Riemann zeta function. The derivations of the coefficients can be found in the review of Loos and Gill [20]. The coefficients  $f_0, f_1$  and  $f_2$  were taken from Sun, Perdew and Seidl [9].

W20	
$a_0(0)$	$(1-\ln 2)/\pi^2$
$b_0(0)$	$-0.071100 + \frac{\ln 2}{6} - \frac{3}{4\pi^2} z(3)$
$a_1(0)$	$(\frac{9\pi}{4})^{-1/3} \frac{1}{4\pi^3} (\frac{7\pi^2}{6} - 12\ln 2 - 1)$
$b_1(0)$	-0.01
$a_0(1)$	$\frac{(1-\ln 2)}{2\pi^2}$
$b_0(1)$	$-0.049917 + \frac{\ln 2}{6} - \frac{3}{4\pi^2} z(3)$
$a_1(1)$	$2^{-4/3} (\frac{9\pi}{4})^{-1/3} \frac{1}{4\pi^3} (\frac{13\pi^2}{12} - 12\ln 2 + \frac{1}{2})$
$f_0$	-0.9
$f_1$	1.5
$f_2$	0
$c_x[0]$	$-\frac{3}{4\pi} (\frac{9\pi}{4})^{1/3}$
$c_s[0]$	$\frac{3}{10} (\frac{9\pi}{4})^{2/3}$
$c_x[1]$	$-2^{1/3} \frac{3}{4\pi} (\frac{9\pi}{4})^{1/3}$
$c_s[1]$	$2^{2/3} \frac{3}{10} (\frac{9\pi}{4})^{2/3}$

TABLE II. Correlation energies per electron (in eV) for UEG from C16 [13], revC16 [18], W20, and QMC data of Spink *et al.* [12].

$\zeta$	$r_s$	Spink <i>et al.</i>	C16	revC16	W20
$\zeta=0$	1.0	-1.605	-1.580	-1.593	-1.621
	2.0	-1.218	-1.182	-1.198	-1.212
	3.0	-1.010	-0.978	-0.995	-1.003
	5.0	-0.774	-0.752	-0.769	-0.772
	10.0	-0.510	-0.499	-0.515	-0.513
	20.0	-0.316	-0.309	-0.321	-0.317
$\zeta=0.34$	1.0	-1.550	-1.507	-1.519	-1.545
	2.0	-1.170	-1.129	-1.144	-1.156
	3.0	-0.969	-0.935	-0.951	-0.958
	5.0	-0.741	-0.719	-0.736	-0.737
	10.0	-0.489	-0.478	-0.493	-0.491
	20.0	-0.303	-0.297	-0.309	-0.304
$\zeta=0.66$	1.0	-1.325	-1.296	-1.305	-1.324
	2.0	-1.014	-0.974	-0.986	-0.994
	3.0	-0.841	-0.809	-0.822	-0.826
	5.0	-0.645	-0.625	-0.638	-0.638
	10.0	-0.427	-0.419	-0.431	-0.427
	20.0	-0.267	-0.262	-0.271	-0.266
$\zeta=1$	1.0	-0.827	-0.851	-0.854	-0.859
	2.0	-0.642	-0.650	-0.654	-0.654
	3.0	-0.537	-0.546	-0.550	-0.548
	5.0	-0.420	-0.428	-0.434	-0.430
	10.0	-0.287	-0.294	-0.299	-0.293
	20.0	-0.186	-0.189	-0.193	-0.186

TABLE III. Statistical summary of errors (in eV) of seven UEG correlation functionals against the QMC results ( $1 \leq r_s \leq 20$ ) of Spink *et al.* [12]. The statistical errors for PZ81, PW92, and DPI were computed by using the raw data in the work of Bhattacharai [11]. MSE = mean signed error = mean signed deviation; MUE = mean unsigned error = mean absolute deviation.

	$\zeta = 0$		$\zeta = 0.34$		$\zeta = 0.66$		$\zeta = 1$		AMUE
	MSE	MUE	MSE	MUE	MSE	MUE	MSE	MUE	
PZ81	-0.003	0.007	0.000	0.005	0.007	0.007	-0.010	0.011	0.007
W20	-0.001	0.006	0.000	0.012	0.007	0.007	-0.012	0.012	0.009
PW92	0.000	0.007	-0.007	0.013	-0.006	0.010	-0.007	0.008	0.010
VWN80	-0.001	0.008	-0.011	0.016	-0.011	0.011	-0.007	0.007	0.011
revC16	0.007	0.010	0.014	0.015	0.011	0.014	-0.014	0.014	0.013
DPI	0.005	0.015	-0.008	0.025	-0.002	0.018	-0.005	0.012	0.018
C16	0.023	0.023	0.028	0.028	0.022	0.022	-0.010	0.010	0.020